



# Monitoring climate sensitivity shifts in tree-rings of eastern boreal North America using model-data comparison

Clémentine Ols, Martin P. Girardin, Annika Hofgaard, Yves Bergeron, Igor Drobyshev

## ► To cite this version:

Clémentine Ols, Martin P. Girardin, Annika Hofgaard, Yves Bergeron, Igor Drobyshev. Monitoring climate sensitivity shifts in tree-rings of eastern boreal North America using model-data comparison: Shifts in tree growth sensitivity to climate. *Ecosystems*, 2017, 10.1007/s10021-017-0203-3 . hal-01435349

**HAL Id: hal-01435349**

**<https://hal.science/hal-01435349>**

Submitted on 8 Dec 2017

**HAL** is a multi-disciplinary open access archive for the deposit and dissemination of scientific research documents, whether they are published or not. The documents may come from teaching and research institutions in France or abroad, or from public or private research centers.

L'archive ouverte pluridisciplinaire **HAL**, est destinée au dépôt et à la diffusion de documents scientifiques de niveau recherche, publiés ou non, émanant des établissements d'enseignement et de recherche français ou étrangers, des laboratoires publics ou privés.

Public Domain

**Monitoring climate sensitivity shifts in tree-rings of eastern boreal North America using model-data comparison**

Clémentine Ols<sup>1,2\*</sup>, Martin P. Girardin<sup>3</sup>, Annika Hofgaard<sup>4</sup>, Yves Bergeron<sup>1</sup> & Igor Drobyshev<sup>1,5</sup>

1- Institut de recherche sur les forêts, Université du Québec en Abitibi-Témiscamingue, 445  
boul. de l'Université, Rouyn-Noranda, QC J9X 5E4, Canada

2- Institut National de l'Information Géographique et Forestière, Laboratoire d'Inventaire  
Forestier, 14 rue Girardet, 54000 Nancy, France

3- Natural Resources Canada, Canadian Forest Service, Laurentian Forestry Centre, 1055 du  
P.E.P.S., P.O. Box 10380, Stn. Sainte-Foy, Quebec, QC G1V 4C7, Canada

4- Norwegian Institute for Nature Research, P.O. Box 5685 Sluppen, NO-7485, Trondheim,  
Norway

5- Southern Swedish Forest Research Centre, Swedish University of Agricultural Sciences, P.O.  
Box 49, SE-230 53, Alnarp, Sweden

Clementine Ols, \*Corresponding author, (1) [clementine.ols@ign.fr](mailto:clementine.ols@ign.fr), (2) [clementine.ols@uqat.ca](mailto:clementine.ols@uqat.ca), :  
+33782818920

Martin P. Girardin, [martin.girardin@canada.ca](mailto:martin.girardin@canada.ca)

Annika Hofgaard, [annika.hofgaard@nina.no](mailto:annika.hofgaard@nina.no)

Yves Bergeron, [yves.bergeron@uqat.ca](mailto:yves.bergeron@uqat.ca)

Igor Drobyshev, (1) [igor.drobyshev@uqat.ca](mailto:igor.drobyshev@uqat.ca), (2) [igor.drobyshev@slu.se](mailto:igor.drobyshev@slu.se)

For author contributions see footnote below<sup>1</sup>

Keywords: boreal forests, North America, forest growth models, climate change, climate-growth  
relationships, black spruce, *Picea mariana*

---

C.O., M.P.G. and I.D. designed research; C.O. and M.P.G. performed research; C.O. and M.P.G.  
contributed new analytic tools; C.O. and M.P.G. analyzed data; and C.O., M.P.G., I.D., A.H., and Y.B.  
wrote the paper.

Abstract

The growth of high-latitude temperature-limited boreal forest ecosystems is projected to become more constrained by soil water availability with continued warming. The purpose of this study was to document ongoing shifts in tree growth sensitivity to the evolving local climate in unmanaged black spruce (*Picea mariana* (Miller) B.S.P.) forests of eastern boreal North America (49°N-52°N, 58°W-82°W) using a comparative study of field and modeled data. We investigated growth relationships to climate (gridded monthly data) from observed (50 site tree-ring width chronologies) and simulated growth data (stand-level forest growth model) over 1908-2013. No clear strengthening of moisture control over tree growth in recent decades was detected. Despite climate warming, photosynthesis (main driver of the forest growth model) and xylem production (main driver of radial growth) have remained temperature-limited. Analyses revealed, however, a weakening of the influence of growing season temperature on growth during the mid- to late-20<sup>th</sup> century in the observed data, particularly in high-latitude (> 51.5 °N) mountainous sites. This shift was absent from simulated data, which resulted in clear model-data desynchronization. Thorough investigations revealed that desynchronization was mostly linked to the quality of climate data, with precipitation data being of particular concern. The scarce network of weather stations over eastern boreal North America (> 51.5 °N) affects the accuracy of estimated local climate variability and critically limits our ability to detect climate change effects on high-latitude ecosystems, especially when drought severity is projected to rise. Climate estimates from remote sensing could help address some of these issues in the future.

## Introduction

Tree growth rates are well correlated with spatial and temporal climate variability (Gifford and Evans 1981; Rennenberg and others 2006; Wu and others 2012; Vlam and others 2014; Gričar and others 2015). Since the beginning of the Industrial Revolution, increasing anthropogenic activities have altered global climate and local weather dynamics, particularly during the last century (Mann and others 1998; IPCC 2014), thereby affecting tree growth processes. Tree growth in many boreal regions lost its positive response to rising temperatures during the late-20<sup>th</sup> century (D'Arrigo and others 2008), a phenomenon often paralleling increased sensitivity of tree growth to precipitation and drought severity (Buermann and others 2014; Galván and others 2015; Latte and others 2015). Yet causes for changing climate sensitivity in tree-rings vary and may also result from responses to other phenomena that are associated with changing cloud cover, delayed snowmelt and increasing local pollution (Vaganov and others 1999; D'Arrigo and others 2008). Furthermore, links between temporal variations in tree responses to climate and climate change likely involve cross-scale interactions between abiotic and biotic variables, e.g., tree age/size and site characteristic effects on tree growth (Carrer and Urbinati 2004; Rossi and others 2008; Ibáñez and others 2014; Navarro-Cerrillo and others 2014) and insect herbivory (Krause and others 2012; Fierravanti and others 2015). The evaluation of climate change effects on tree growth dynamics remains challenging (Girardin and others 2016b).

In the boreal forest of eastern North America, seasonal temperatures have increased by as much as 3°C since the beginning of the 20<sup>th</sup> century (Hansen and others 2010; Jaume-Santero and others 2016), while seasonal precipitation has shown variable patterns (Wang and others 2014). Studies have reported a decrease in tree growth sensitivity to growing season temperature in historically 'temperature-limited' high latitude and high altitude forests (Jacoby and D'Arrigo 1995; Briffa and others 1998; Galván and others 2015). In parallel, growth declines have been reported over the late 20<sup>th</sup> century (Girardin and others 2016a), while the occurrence of years with extremely low growth in the boreal forest of eastern North America has increased throughout the 20<sup>th</sup> century (Ols and others 2016). Both phenomena have been attributed to increased drought impacts on tree growth. During the 21st century, soil water availability, atmospheric water demand and heat stress in the boreal forest of

eastern North America are projected to limit tree growth increasingly as a consequence of continuing warming (Girardin and others 2016b; Novick and others 2016). The degree to which this forest will adapt to warmer and drier conditions, e.g., by increasing its water use efficiency, is uncertain (Charney and others 2016). Therefore, it is important that these ecosystems are continuously monitored to detect early warning signs of changes in climatic controls on tree growth (Gauthier and others 2015). However, such observation-based monitoring is complicated by the large spatial extent of the boreal forest of eastern North America.

Forest growth models can facilitate the exploration of tree growth processes and their expected relationships with the evolving local climate. Such models can be built upon sets of mathematical equations accounting for non-linear relationships between specific environmental and physiological variables that have been derived from empirical observations (Landsberg and Waring 1997; Misson 2004). Studying the coherency of climatic signals that are contained in empirical tree growth data and simulated tree-growth data may help us understand whether variations in tree-growth responses to climate emerge from changing climate alone or from changes in tree-growth sensitivity to climate. Modeling may also help the study of tree growth and its sensitivity to climate in areas where ground sampling is more difficult due to the remoteness of locations and the costs that are associated with this type of sampling.

In this study, we explore the possibilities of detecting shifts in tree growth sensitivity to climate in boreal black spruce forests of eastern North America by comparing observed and model-based climate-growth relationships over the period 1908-2013. Through this case study, we have proposed an experimental design that could be paired with ongoing national forest inventory programs (e.g., Girardin and others 2016a) to implement large-scale, systematic and long-term monitoring of tree growth sensitivity to climatic variations. Here, observed data consisted of a newly acquired network of 50 annually resolved and absolutely dated black spruce tree-ring width chronologies covering latitudinal and longitudinal gradients of eastern boreal North America (49°N-52°N, 58°W-82°W, Fig. 1). Regarding the model-based data, we used a stand-level forest growth model that was based on the Physiological Principle Predicting Growth (3PG) model (Landsberg and Waring 1997) to simulate yearly site-specific net primary production (NPP) for the period encompassing the observed data (i.e.,

1908-2013). Two hypotheses were formulated on the basis of the widely accepted evidence that temperatures have been rising in the study region:

(H1) Yearly variability in tree growth is under the control of climate. The validity of this hypothesis implies a significant correlation between tree-ring width data and climatically driven simulations of NPP;

(H2) The control of water on tree growth has increased over time along with the rise of temperature, particularly in high-latitude and high-altitude forests. This implies an increased positive sensitivity to precipitation, in both tree-ring width data and climatically driven simulations of NPP.

## **Material and methods**

### *Study area*

The study area consists of three latitudinal transects (western, central and eastern; Fig. 1a) that were established in northern boreal Quebec (Ols and others 2016). The terrain in this area is characterized by low plains in the west (200-350 m above sea level [a.s.l.]) and by mountains, where topographic relief is particularly pronounced in the north, central and eastern regions (up to 1128 m a.s.l. in the Otish Mountains). The two main climatic gradients in the study area are a decreasing temperature gradient from south to north and an increasing summer (June to August) precipitation gradient from west to east (Fig. 1b). The eastern region is regularly prone to spruce budworm (*Choristoneura fumiferana* [Clemens]) outbreaks (Boulanger and Arseneault 2004).

### *Tree-ring width measurements*

Tree growth data ( $n = 890$  trees) were collected at 50 sites that were located along the three latitudinal transects (Fig. 1a; Table S1) (Ols and others 2016). All sites were pure, unmanaged old-growth black spruce (*Picea mariana* (Miller) B.S.P.) forests growing on xeric to meso-xeric soils (Direction des inventaires forestiers 2015). Between 10 and 27 dominant trees (standing living or dead) were sampled per site (one core per tree). Sampled cores were processed using standard procedures and the rings were visually and statistically cross-dated. Tree-ring width measurements were detrended using a 60-year spline to eliminate noise that was caused by site- and biologically related effects (e.g.,

competition, self-thinning and aging) (Cook and Peters 1997). Detrended ring-width measurements were then processed using autoregressive modeling to remove autocorrelation (pre-whitening) and averaged into site-specific residual tree-ring width (RWI) chronologies using a robust bi-weighted mean.

#### *Climate data*

Climatological data that were used as inputs to the forest growth model and in the calculations of climate-growth relationships were monthly means of maximum ( $T_{\max}$ ) and minimum ( $T_{\min}$ ) temperatures, and monthly total precipitation (Prec), which were all extracted from the  $0.5^\circ \times 0.5^\circ$  CRU TS 3.22 database (Harris and others 2014). The climatic characteristics of each study site were extracted over the 1901-2013 period, using a site-centered  $0.5^\circ \times 0.5^\circ$  grid cell. We retrieved data from twenty-one grid cells, with each grid cell containing between 1 and 7 study sites. Consequently, some study sites exhibited identical climatic characteristics (Table S1). To test the influence of climate data type on model simulations and climate-growth relationships, site-specific climate data ( $T_{\min}$ ,  $T_{\max}$  and Prec) were also extracted over the 1901-2013 period (using the same procedures as above) from three alternative databases: (1) the Canadian software BioSIM (Régnière and others 2014); (2) the combined  $0.5^\circ \times 0.5^\circ$  CRU TS 3.22 temperature (Harris and others 2014) and GPCC precipitation (Full Data Reanalysis Version 7, Schneider and others 2015); and (3) Twentieth Century Reanalysis (20CR, Compo and others 2011) datasets. The 20CR data are derived from oceanic temperature and surface pressure data, and do not incorporate precipitation and station temperature records (Compo and others 2011); 20CR may thus be viewed as being independent of all other climate products.

The boreal region of eastern Canada is not covered by a dense network of weather stations (Fig. S1). In many instances, the existing stations have been running intermittently (Girardin and others 2016b). To capture precipitation and temperature input data accuracy through space and time, the number and location of meteorological stations that were used for climatic interpolations within our study area were extracted. We also extracted the only long-running hydrological record that was available for the study area, i.e., the 1960-1993 De Pontois river flow from HYDAT 28.0 (Water Survey of Canada, <http://www.ec.gc.ca/rhc-wsc>) (Table S3), and used this record as a surrogate for

drought conditions (Haslinger and others 2014).

*Forest attributes*

Biometric information necessary for the model simulation was obtained as follows. First, the above-ground biomass in Mg per hectare ( $W_{abg}$ ) was estimated at each study site using country-wide species-specific allometric equations (Paré and others 2013) that were applied to site-specific basal areas (Table S2). Second, site-specific topography data (slope and aspect values; Table S2) were extracted from Canada 3D, a digital elevation model (DEM) that was produced by the Canadian Forestry Service (Natural Resources Canada 2002) using ArcGIS® (ESRI 2011). Last, historical patterns of defoliation severity that was incurred by the spruce budworm (1967–2016), and which were compiled from Quebec’s annual provincial surveys (Ministère des Forêts, de la Faune et des Parcs du Québec [MFFPQ] 2014), were extracted for each of our sites.

*Net primary productivity data*

Net primary production (NPP) at our 50 sites was simulated using the StandLEAP model (version 0.1 SVN, Girardin and others 2016b). StandLEAP is a generalized plot-level model that is based upon the 3PG model (Landsberg and Waring 1997), which is applicable to relatively homogeneous forests. It was developed for the estimation of forest productivity over large areas (e.g., Girardin and others 2016b) but with a spatial resolution that was sufficiently fine for use in forest management (e.g., Raulier and others 2000; Coulombe and others 2009; Anyomi and others 2014). StandLEAP can be parameterized for individual species and its application to any stand does not require fine-tuning of the model to fit the data. The model has been tested against numerous independent tree-ring datasets in western, central and eastern Canada (Girardin and others 2008, 2011b, 2011a, 2012, 2014, 2016b). StandLEAP runs on a monthly time-step. In StandLEAP, parameters are set up to fully characterize the effects of many interacting and non-linear modifiers of carbon flux quantities (e.g., growth and respiration). Absorbed photosynthetically active radiation (APAR) is related to growth primary production (GPP) using a radiation use efficiency (RUE) coefficient that differs among locations and through time as a function of environmental constraints. Constraints take the form of species-specific



parameters ( $f_1, \dots, f_n$ ) that take a value of 1 under average conditions; they are closer to zero to represent increasing limitations, or above 1 as conditions improve towards optimal. Constraints represent the effects of soil drought (Bernier and others 2002), frost (Aber and others 1996) (both limited to a maximum of 1.0), mean maximum and minimum air temperature, vapor pressure deficit (VPD), radiation, and leaf area index (where values greater than 1.0 are possible) on GPP. The following equation summarizes these functions:

$$GPP = APAR \times (\overline{RUE} \times f_1 f_2 \dots f_n), \quad (1)$$

where  $\overline{RUE}$  represents a species-specific mean value of RUE that is applicable to the entire species' range. Monthly canopy light absorption and photosynthesis parameters were derived from metadata that were generated using a more detailed multi-layer, hourly time-step model of canopy photosynthesis and transpiration that is called FineLEAP (Raulier and others 2000; Hall and others 2006). Representation of photosynthesis in FineLEAP is based upon the equations of Farquhar and others (1980). Additional details of the procedure and origin of the basic field measurements and procedure for estimation of parameters for radiation interception, radiation- and water-use-efficiency can be found in Hall and others (2006). NPP is computed monthly, after partitioning respiration into maintenance ( $R_m$ ) and growth ( $R_g$ : a fixed proportion of the difference between GPP and  $R_m$ ) quantities and subtracting these from GPP. Maintenance respiration is computed as a function of temperature using a  $Q_{10}$  relationship (Ågren and Axelsson 1980; Ryan 1991; Lavigne and Ryan 1997). Acclimation of respiration to temperature is modelled using the equation of Smith and others (2016). As is the case in 3-PG, part of NPP is first allocated to fine roots (Eq. (13) in Landsberg and Waring 1997) on a yearly basis and then to replacement of carbon biomass that is lost to leaf and fine woody litter turnover. The remaining NPP is then allocated to increments in stand carbon compartments of foliage, branches, coarse roots and stems. The modifier for soil water availability is based on modeled water balance, which is coupled to transpiration and NPP, as described by Bernier and others (2002). The impact of  $CO_2$  fertilization is included through a modifier of the potential water use efficiency (WUE), as described by Girardin and others (2016b). The active soil depth was set to 600mm at all sites (Table S2). An active soil depth between 300 and 900mm has generally been accepted as a

desirable range for black spruce (Viereck and Johnston 1990; Girardin and others 2016b). Three sites (viz., 39, 45 and 47; Table S2) had their above-ground biomass truncated to a maximum value of 110 Mg/ha because of estimated field values that reached higher than typical conditions for which the model was calibrated. All carbon flux quantities used in this study were made insensitive to changing forest age over time, by fixing constant forest attributes (e.g., biomass and stem densities) across all simulation years. Carbon flux quantities solely express direct climate influences on plant growth, avoiding the influence of post-fire stand dynamics on fluxes (e.g., Girardin and others 2011a; Pan and others 2011) and allowing a direct comparison with climate driven tree-ring width measurements that were collected from old-growth forest stands. The model does not simulate soil processes other than water balance, since it implicitly assumes constant soil nutrient properties and turnover. Furthermore, computations assume the absence of insect outbreaks.

#### *Correlation between tree-ring and NPP metrics*

Carry-over effects from the previous growing season have been reported to affect tree growth significantly the following season, and particularly in harsh environments (Babst and others 2014; Ols and others 2016). For instance, lower carbohydrate reserves in the following growing season, can notably decrease the capacity of trees to respond to favorable growth conditions. Accordingly, monthly NPP values that were obtained from modelling were summed from July of the previous year to June of the current year of growth to represent carbon quantities that were mobilized and allocated to growth from one year to the next (as in Girardin and others 2016b). The correspondence between annual RWI and NPP metrics were then explored through moving window correlations (one-tailed test) at site level. Correlations were computed in R (R Core Team 2015) using 21-year-long windows that were incremented in five-year steps from 1908 to 2013. The null hypothesis of no positive correlation between RWI and NPP was rejected when  $P < 0.05$ . Temporal stability in correlations between RWI and NPP metrics were also investigated at the regional level using the same moving-correlation procedure as above. Regional RWI and NPP metrics were computed as a robust bi-weighted mean of all site-specific metrics. The significance of each 21-year correlation averaged across sites was evaluated using a competitive test, which combines the probabilities of dependent

tests using Fisher's method (Dai and others 2014). When applied to our specific case, it compares, for each 21-year period the distribution of  $P$  values of all site-specific NPP and RWI correlations to the distribution of randomly selected 100,000 vectors of  $P$ -values of similar length. Competitive tests were computed in R using the *competitive.test* function that is available in the *CombinePValue* package (Dai 2014). To test for coherence in year-to-year variability between the two metrics, moving correlations between first-differenced RWI and NPP metrics (subtraction of the value at year<sub>t-1</sub> from the value at year<sub>t</sub>) were also computed using the same methodology that was described above.

#### *Climate-growth relationships*

Coherency in the climatic signals that were contained in RWI and NPP metrics were investigated by correlation analyses. First, correlations between tree-growth metrics and monthly climate data were computed using 21-year-long windows incremented in five-year steps from 1908 to 2013 using the *treeclim* package (Zang and Biondi 2015). Climate data included monthly maximum and minimum temperatures and monthly total precipitation. Months spanned from May of the previous year to August of the current year of growth. Site-specific moving correlations were then averaged across all sites to characterize monthly climate-growth relationships at the scale of our study area. The following hypotheses, which were based upon the earlier work by Girardin and others (2016b), were postulated and tested using one-tailed tests: (1) growth is positively correlated with previous September through current May (hereafter September-May) temperatures; (2) growth is negatively correlated with June-August temperatures; and (3) growth is positively correlated with precipitation, regardless of the month. Alternatively, we also tested the inverse versions of hypotheses 1 to 3: (4) growth is negatively correlated with September-May temperatures; (5) positively correlated with June-August temperatures; and (6) negatively correlated with precipitation. Hypotheses 1-6 were considered true both for months of the previous year and current growing season. These procedures were run for both RWI and NPP series. Note that stronger correlations observed with NPP can logically emerge from computation alone, since NPP is itself computed from these climate data. The significance of each 21-year correlation averaged across sites was evaluated using the competitive test that was described earlier. We opted for six one-tailed hypotheses rather than three two-tailed hypotheses, because under

two-sided testing the analysis is particularly sensitive when both strong positive and negative effects occur across sites (Whitlock 2005). Last, the distributions of site-specific correlations with monthly climate variables of the two metrics were compared using Wilcoxon-Mann-Whitney (U-test) and Kolmogorov-Smirnov tests. To test for coherence between local drought conditions and forest growth, we also computed the correlation between tree growth metrics and the mean July-to-September De Pontois river flow, using both raw and first-differenced metrics.

## Results

### *Climate sensitivities in tree growth metrics*

RWI was generally positively correlated with current year spring and summer temperatures (Fig. 2a). However, these correlations decreased substantially and became non-significant during the mid- to late-20<sup>th</sup> century (Fig. 2a). This decrease in correlation corresponded with the emergence of significant negative correlations with previous summer and previous October temperatures (maxima and minima) from the 1940s to 1990s, and with current spring precipitation during a brief period covering the 1960s to 1980s (Fig. 2a). In addition, significant positive correlations between RWI and early winter temperatures were observed during the late-20<sup>th</sup> century (Fig. 2a). The correlation between RWI metrics and the mean July-to-September De Pontois river flow of the year prior to growth, and over the period 1960-1993, was significantly positive (median correlation:  $r = 0.31$ ), especially at high latitudes ( $> 51.5^\circ\text{N}$ ) (Fig. 3). In summary, annual growth variability in this boreal region of eastern North America has shifted from being positively correlated with growing-season temperature early in the 20<sup>th</sup> century, to being negatively correlated with summer temperature during mid-century, and then back to being positively correlated with temperature during the late-20<sup>th</sup> century. There was no clear evidence of a strengthening of tree growth sensitivity to precipitation throughout the 1908-2013 period, using CRU precipitation data (Fig. 2a).

Relationships between NPP and monthly climate variables were similar to those observed for RWI metrics (Fig. 2b, c). NPP correlated positively with current year temperatures, but this relationship was much weaker from 1958 to 1988 compared to all other periods (Fig. 2b). Between 1973 and 1998, there was an emergence of significant negative correlations with previous summer

temperature (Fig. 2b). Unlike RWI, there was a period of sustained significant positive correlations with July or August precipitation during the year contemporaneous to growth from 1933 to 1998 (Fig. 2b). Wilcoxon-Mann-Whitney tests indicated that the distribution of correlations between NPP and monthly temperature (minimum and maximum) was generally more homogeneous than with RWI (Fig. 2c). In contrast, the distributions of correlations with precipitation for both metrics were mostly similar. This was also observed using Kolmogorov-Smirnov tests (Fig. S2). NPP metrics and the mean July-to-September De Pontois river flow were not significantly correlated ( $P > 0.05$ ) (data not shown). However, these variables were significantly correlated after a first-difference transformation in 33 of the 50 study sites, mostly north of 51.5°N and west of 74.0°W (median correlation:  $r = 0.32$ ; correlation pattern was similar to the RWI pattern exhibited in Fig. 3d, but with both variables taken on their non-lagged calendar years; results not shown). In summary, NPP variability shifted from being temperature-driven in the early-20<sup>th</sup> century (an indication of temperature limitation of the rate of photosynthesis), to precipitation-driven during the mid- to late-20<sup>th</sup> century (i.e., the influence of available moisture), and then again temperature-driven during the late-20<sup>th</sup> century.

#### *Synchronicity in tree growth metrics*

Correlations between site-specific RWI and NPP metrics at the regional level were often positive and significant during the early-20<sup>th</sup> century, and throughout the late-20<sup>th</sup> to early-21<sup>st</sup> centuries (Fig. 4). However, a clear desynchronization was observed in the middle of the century at almost all sites, when correlations substantially decreased to become negative and occasionally significantly negative (Fig. 5, left-hand panels). Although its duration and timing differed across sites, this desynchronization was most prominent in mountainous north easternmost sites (Fig. 6d), i.e., in areas ongoing the most rapid warming (Fig. 1a). First-differencing of the RWI and NPP data enhanced correlations during the late-20<sup>th</sup> century but decreased correlations during the early-20<sup>th</sup> century across the whole area (Fig. 5, right-hand panels). It is noteworthy that the same mid- to late-20<sup>th</sup> century desynchronization between observed and simulated tree-growth metrics was obtained using alternative climate datasets, albeit with variations in the onset and duration of this desynchronization depending upon the data products (Fig. S3). For instance, correlations between NPP and RWI were improved during the 1933-1963

period when fed by simulations of NPP that were driven by the 20CR data, although they did not fully compensate for model-data desynchronization (Fig. S3d).

## Discussion

The purpose of this study was to document shifts in tree growth sensitivity to climate in temperature-limited boreal forest ecosystems of eastern boreal North America over 1908-2013 using a comparative study of field and modeled data.

Despite climate warming in the study area (Figs. 1a and S4), there was no clear evidence for a strengthening of radial tree growth (RWI) sensitivity to precipitation during recent decades (Fig. 2). The post-1980 significant positive correlations between (1) growing-season temperature and radial growth (Fig. 2c), and between (2) radial growth and modeled productivity (NPP) across the entire study region (Fig. 4) indicate that both photosynthesis (the main driver of the model) and xylem formation (the main driver of radial growth) have until recently remained temperature-limited. The response of tree radial growth in our study area is therefore different from the response that has been frequently reported in the literature for the boreal forest. A likely reason for this lack of increased sensitivity in tree growth to precipitation may be that despite rising temperature (Fig. 1a), atmospheric water demand may have decreased over the course of the 20<sup>th</sup> century in our study area (Fig. S5; also see Fig. S9 in Girardin and others 2016b). A decrease in water demand, coupled with a potential increase in water use efficiency under elevated atmospheric CO<sub>2</sub> concentrations, may have contributed to the stabilization of tree dependence upon incoming precipitation that is necessary for soil moisture recharge.

Our results revealed that while modeled productivity remained somewhat spring temperature-sensitive over the entire study period, the positive influence of growing season temperature on radial growth briefly disappeared during the mid-20<sup>th</sup> century. This phenomenon occurred in parallel with an increased sensitivity to moisture, as indicated by the negative correlation between radial growth and summer temperature, by the positive correlation between radial growth and the mean July-to-September De Pontois river flow, and by the positive correlation between modeled productivity and July precipitation. During this same period, the overall region-wide significant synchrony between

modeled productivity and radial growth also dropped to become insignificant, particularly at eastern high-latitude mountainous sites, i.e., those undergoing the strongest warming (Fig. 1a). This sudden model-data desynchronization is noteworthy and deserves attention, as it may impair our capacity to monitor shifts in tree growth sensitivity to climate in these forests. We subsequently discuss three factors that may be involved in this desynchronization: accuracy of input climate data; the advent of external factors in the ecosystem; and model uncertainties.

Climate data uncertainties have a large influence on model-based estimations of historical and ongoing ecosystem processes. The choice of climate dataset, with those of precipitation being of particular concern, affects the capacity to identify drivers of variability in empirical data products and model results (e.g., Daly and others 1994; Ito and others 2017; Wu and others 2017). For example, the probability of a false negative result (e.g., a significant RWI-precipitation correlation that was not detected when a true relationship exists) could theoretically be higher at sites where climate data quality is lowest (Wilson and others 2007). In the current study, the quality of climate data is likely to be a critical factor explaining the drop in model-data correspondence during the mid- to late-20<sup>th</sup> century. First, the desynchronization in model-data correspondence was most prominent at sites located above 51.5 °N (Fig. 5c), i.e., where station density is low (Figs. 5 and S1). Therefore; there is an apparent relationship between station density and climate signal degradation. Additionally, weak model-data correspondence was clearly linked to altitudinal differences between reference stations (mainly located along the coast) and mountainous sampled sites, with a higher capacity to detect a positive correlation between radial growth and modeled productivity at low altitude sampling locations (Fig. 6d). This bias finds explanation in the fact that CRU temperature interpolations over eastern North America do not depict altitudinal climate gradients (Fig. S6). Our capacity to model forest growth in mountainous regions is thus very likely hindered by inaccuracies of temperature and precipitation estimates at these high-altitude sites. The variations in the onset and duration of the desynchronization between radial growth and modeled productivity across climate data products illustrate the problem of climate data uncertainties, which are particularly present in precipitation estimates (Figs. S1c and S7). Cross-correlations between CRU and the 20th Century Reanalysis (20CR) precipitation gridded data show strong inconsistencies during the period 1940-1980 (Fig. S7).

This pinpoints a significant error in data estimation in one or the other climatic product, or both. It is noteworthy that the onset of desynchronization between radial growth and modeled productivity coincides with a period of high weather station density in the region (Fig. 6a). Yet, many of these stations have recorded observations intermittently, which can be observed from the fluctuations in the annual number of stations contributing to the climate interpolation algorithm (Fig. S1b&c).

Outbreaks of eastern spruce budworm, which are recurrent in the boreal forest of eastern North America but currently not accounted for during simulations, could have contaminated field data by disrupting radial growth responses to local climate, thereby causing the model-data desynchronization (Girardin and others 2016b). We did not observe any obvious abrupt growth decline or release, which is typical of severe outbreak defoliation on these site chronologies (Figs. 4 and S7). Also, most of the sites showing desynchronization were located in an area that did not show historical evidence of spruce budworm outbreaks during the periods of 1947-1958, 1975-1992 and 2007-2016 (Fig. 6b). Furthermore, the sampled stands were free of the main budworm host-species *Abies balsamea* (L.) Miller. Although the influence of such disturbance on growth cannot be ruled out entirely, its role in the observed model-data desynchronization can be only minor. It may, however, become an important concern if this experimental design is to be applied in regions where this disturbance is recurrent (Girardin and others 2016b).

Our experimental design assumes that radial growth and modeled productivity are directly comparable analogs. However, this disregards documented evidences that shifts in radial growth sensitivity, to temperature for instance, emerge from changes in allocation of assimilates within a tree (Lapenis and others 2013). Assimilate allocation is strongly sensitive to stand density (e.g., denser stands favoring allocation to terminal buds to increase access to light) and climate (e.g., drier climate favoring allocation to roots to increase access to water). The period of desynchronization was characterized by a decrease in spring precipitation and an increase in spring temperature (Fig. S4). Such climatic conditions may have temporarily favored the allocation of assimilates to the root system against radial growth, disrupting radial growth responses to climate. In a sensitivity analysis where the productivity fraction allocated to the stem was substituted for total annual productivity (as in Girardin and others 2008), we noted an improved model-data correspondence during the first half (1940-1960) of the



desynchronization period (Fig. S9). Yet the correspondence deteriorated substantially during the second half (1960-1980) (Fig. S9). Moreover, many of the sites showing model-data desynchronization were located in open-canopy stands adjacent to the limit between spruce-moss and spruce-lichen domains, which were located north of 51.5°N (Robitaille and Saucier 1998). Thus, there are no reasons to believe that height growth would have been favored over diameter growth during the mid- to late-20<sup>th</sup> century. Model-data desynchronization during the mid- to late-20<sup>th</sup> century, therefore, does not appear to be linked to shifts in field growth allocation patterns.

Finally, the formulation of the model used herein may be missing important dynamic processes that are associated with snow accumulation and thawing, initiation of leaf-out and growth processes. The sudden negative sensitivity to spring precipitation in radial growth over the mid- to late-20<sup>th</sup> century, which was not observed with modeled productivity, may be indicative of a stronger negative impact of spring precipitation on tree growth (Huang and others 2010; Girard and others 2011; Ols and others 2016). Sites exhibiting a sudden negative sensitivity to spring precipitation were the ones undergoing the strongest warming (Fig. 1a) and were mainly located in high-altitude mountainous areas (Fig. 6d). Snow dynamics (snowfall and snowmelt) influence tree growth and climate-growth relationships at boreal latitudes (Frechette and others 2011; Verbyla 2015), particularly along altitudinal gradients (Trujillo and others 2012). Indeed, a thick spring snow cover may delay the start of the growing season through delayed snow melt (Vaganov and others 1999). The current formulation of the water balance within the model does not include a dynamic snow model, as is the case in Terrier and others (2013). This may mask the onset and duration of the drought season, and ultimately, affect the capacity to uncover drivers that are associated with the water balance at high-altitude sites.

## Conclusion

Climate change and its impact on high-latitude boreal ecosystems are now recognized. There is no doubt that, in the near future, intensive efforts will be required to monitor these impacts to pave the way for adaptation and mitigation solutions (Gauthier and others 2015). This will require tools to link ecosystem dynamics adequately to atmospheric properties. In this study, we showed that forest growth

models can reasonably track processes leading to forest growth variability in the northernmost boreal forest of eastern North America through space and time when growth remains temperature-limited (Girardin and others 2008, 2016b). It is conceivable that the analysis proposed here be deployed over larger areas for monitoring, in particular through integration with national forest inventories that specifically aim at providing large-scale systematic, timely and coherent information on the extent, composition and characteristics of forests and their evolution over time (e.g., Girardin and others 2016a). Our work nevertheless illustrated some of the challenges that hinder the capacity to monitor high-latitude boreal ecosystems at fine-scale across a diversity of landscapes. Among various issues, uncertainties in climate data are of particular concern. Many of the temperature-limited regions of boreal Canada are covered by a scarce network of weather stations, which affects the accuracy of local climate variability estimates and that makes it difficult to relate climate to ecosystem dynamics. Availability of climate data, therefore, may critically limit our ability to monitor climate change impacts on high-latitude forest ecosystems while drought severity is projected to rise. Through remote sensing, recent estimates of climate data, notably those of precipitation and snow cover could help address some of these issues in the future.

#### Acknowledgments

We thank Emeline Chaste for GIS analyses, Xiao Jing Guo for assistance with StandLEAP, Williams F. J Parsons for language revision, and two anonymous reviewers and the Associate Editor for helpful comments on an earlier version of this manuscript. This study was funded by the Natural Sciences and Engineering Research Council of Canada (NSERC Strategic and Discovery Grants), the Nordic Forest Research Cooperation Committee (SNS), the Canadian Forest Service (CFS) and the Research Council of Norway (grant 160022/E50). This work was also supported by a fellowship from the Forest Complexity Modelling program (NSERC Strategic and Discovery Grants). The authors have no conflicts of interest to disclose.

## References

- Aber JD, Reich PB, Goulden ML. 1996. Extrapolating leaf CO<sub>2</sub> exchange to the canopy: a generalized model of forest photosynthesis compared with measurements by eddy correlation. *Oecologia* 106:257–265.
- Ågren GI, Axelsson B. 1980. Population respiration: A theoretical approach. *Ecol Model* 11:39–54.
- Anyomi KA, Raulier F, Bergeron Y, Mailly D, Girardin MP. 2014. Spatial and temporal heterogeneity of forest site productivity drivers: a case study within the eastern boreal forests of Canada. *Landsc Ecol* 29:905–918.
- Babst F, Bouriaud O, Papale D, Gielen B, Janssens IA, Nikinmaa E, Ibrom A, Wu J, Bernhofer C, Kostner B, Grunwald T, Seufert G, Ciais P, Frank D. 2014. Above-ground woody carbon sequestration measured from tree rings is coherent with net ecosystem productivity at five eddy-covariance sites. *New Phytol* 201:1289–1303.
- Bernier PY, Bréda N, Granier A, Raulier F, Mathieu F. 2002. Validation of a canopy gas exchange model and derivation of a soil water modifier for transpiration for sugar maple (*Acer saccharum* Marsh.) using sap flow density measurements. *For Ecol Manag* 163:185–96.
- Boulanger Y, Arseneault D. 2004. Spruce budworm outbreaks in eastern Quebec over the last 450 years. *Can J For Res* 34:1035–1043.
- Briffa KR, Schweingruber FH, Jones PD, Osborn TJ, Shiyatov SG, Vaganov EA. 1998. Reduced sensitivity of recent tree-growth to temperature at high northern latitudes. *Nature* 391:678–682.
- Buermann W, Parida B, Jung M, MacDonald GM, Tucker CJ, Reichstein M. 2014. Recent shift in Eurasian boreal forest greening response may be associated with warmer and drier summers. *Geophys Res Lett* 41:1995–2002.
- Carrer M, Urbinati C. 2004. Age-dependent tree-ring growth responses to climate in *Larix decidua* and *Pinus cembra*. *Ecology* 85:730–740.
- Charney ND, Babst F, Poulter B, Record S, Trouet VM, Frank D, Enquist BJ, Evans ME. 2016. Observed forest sensitivity to climate implies large changes in 21st century North American forest growth. *Ecol Lett*. 19:1119–1128

- 490 Compo GP, Whitaker JS, Sardeshmukh PD, Matsui N, Allan RJ, Yin X, Gleason BE, Vose RS,  
491 Rutledge G, Bessemoulin P, Brönnimann S, Brunet M, Crouthamel RI, Grant AN, Groisman  
492 PY, Jones PD, Kruk MC, Kruger AC, Marshall GJ, Maugeri M, Mok HY, Nordli Ø, Ross TF,  
493 Trigo RM, Wang XL, Woodruff SD, Worley SJ. 2011. The Twentieth Century Reanalysis  
494 Project. Q J R Meteorol Soc 137:1–28.
- 495 Cook ER, Peters K. 1997. Calculating unbiased tree-ring indices for the study of climatic and  
496 environmental change. Holocene 7:361–370.
- 497 Coulombe S, Bernier PY, Raulier F. 2009. Uncertainty in detecting climate change impact on the  
498 projected yield of black spruce (*Picea mariana*). Ecol Manage 259:730–738.
- 499 Dai H. 2014. CombinePValue: Combine a vector of correlated p-values. R package version 1.0.  
500 <http://CRAN.R-project.org/package=CombinePValue>
- 501 Dai H, Leeder JS, Cui Y. 2014. A modified generalized Fisher method for combining probabilities  
502 from dependent tests. Front Genet 5:32. doi: 10.3389/gene.2014.00032
- 503 Daly C, Neilson RP, Phillips DL. 1994. A statistical-topographic model for mapping climatological  
504 precipitation over mountainous terrain. J Appl Meteorol 33:140–158.
- 505 D'Arrigo RD, Wilson R, Liepert B, Cherubini P. 2008. On the 'Divergence Problem' in northern  
506 forests: A review of the tree ring evidence and possible causes. Glob Planet Chang 60:289–  
507 305.
- 508 Direction des inventaires forestiers. 2015. Norme de stratification écoforestière - Quatrième inventaire  
509 écoforestier du Québec méridional. Ministère des forêts, de la faune et des parcs.  
510 <https://www.mffp.gouv.qc.ca/forets/inventaire/pdf/norme-stratification.pdf>. Last accessed  
511 09/02/2017
- 512 ESRI. 2011. ArcGIS Desktop: Release 10. Redlands, CA: Environmental Systems Research Institute.
- 513 Farquhar GD, von Caemmerer S, Berry JA. 1980. A biochemical model of photosynthetic CO<sub>2</sub>  
514 assimilation in leaves of C3 species. Planta 149:78–90.
- 515 Fierravanti A, Coccozza C, Palombo C, Rossi S, Deslauriers A, Tognetti R. 2015. Environmental-  
516 mediated relationships between tree growth of black spruce and abundance of spruce  
517 budworm along a latitudinal transect in Quebec, Canada. Agric Meteorol 213:53–63.

- 518 Frechette E, Ensminger I, Bergeron Y, Gessler A, Berninger F. 2011. Will changes in root-zone  
519 temperature in boreal spring affect recovery of photosynthesis in *Picea mariana* and *Populus*  
520 *tremuloides* in a future climate? *Tree Physiol* 31:1204–1216.
- 521 Galván JD, Büntgen U, Ginzler C, Grudd H, Gutiérrez E, Labuhn I, Camarero JJ. 2015. Drought-  
522 induced weakening of growth–temperature associations in high-elevation Iberian pines. *Glob*  
523 *Planet Chang* 124:95–106.
- 524 Gauthier S, Bernier P, Kuuluvainen T, Shvidenko AZ, Schepaschenko DG. 2015. Boreal forest health  
525 and global change. *Science* 349:819–822.
- 526 Gifford RM, Evans LT. 1981. Photosynthesis, carbon partitioning, and yield. *Annu Rev Plant Physiol*  
527 32:485–509.
- 528 Girard F, Payette S, Gagnon R. 2011. Dendroecological analysis of black spruce in lichen—spruce  
529 woodlands of the closed-crown forest zone in eastern Canada. *Ecoscience* 18:279–294.
- 530 Girardin MP, Bernier PY, Gauthier S. 2011a. Increasing potential NEP of eastern boreal North  
531 American forests constrained by decreasing wildfire activity. *Ecosphere* 2: Art. 25, 1–23.
- 532 Girardin MP, Bernier PY, Raulier F, Tardif JC, Conciatori F, Guo XJ. 2011b. Testing for a CO<sub>2</sub>  
533 fertilization effect on growth of Canadian boreal forests. *J Geophys Res* 116:1–16.
- 534 Girardin MP, Bouriaud O, Hogg EH, Kurz W, Zimmermann NE, Metsaranta JM, de Jong R, Frank  
535 DC, Esper J, Büntgen U, Guo XJ, Bhatti J. 2016a. No growth stimulation of Canada’s boreal  
536 forest under half-century of combined warming and CO<sub>2</sub> fertilization. *Proc Natl Acad Sci*  
537 *USA* 113:E8406–E8414.
- 538 Girardin MP, Guo XJ, Bernier PY, Raulier F, Gauthier S. 2012. Changes in growth of pristine boreal  
539 North American forests from 1950 to 2005 driven by landscape demographics and species  
540 traits. *Biogeosciences* 9:2523–2536.
- 541 Girardin MP, Guo XJ, De Jong R, Kinnard C, Bernier P, Raulier F. 2014. Unusual forest growth  
542 decline in boreal North America covaries with the retreat of Arctic sea ice. *Glob Change Biol*  
543 20:851–866.

- 544 Girardin MP, Hogg EH, Bernier PY, Kurz WA, Guo XJ, Cyr G. 2016b. Negative impacts of high  
545 temperatures on growth of black spruce forests intensify with the anticipated climate warming.  
546 *Global Change Biol* 22:627–643.
- 547 Girardin MP, Raulier F, Bernier PY, Tardif JC. 2008. Response of tree growth to a changing climate  
548 in boreal central Canada: A comparison of empirical, process-based, and hybrid modelling  
549 approaches. *Ecol Model* 213:209–228.
- 550 Gričar J, Prislan P, de Luis M, Gryc V, Hacurová J, Vavrčik H, Čufar K.. 2015. Plasticity in variation  
551 of xylem and phloem cell characteristics of Norway spruce under different local conditions.  
552 *Front Plant Sci* 6:730.
- 553 Hall RJ, Raulier F, Price DT, Arseneault E, Bernier PY, Case BS, Guo XJ. 2006. Integrating remote  
554 sensing and climate data with process-based models to map forest productivity within West-  
555 Central Alberta's boreal forest: Ecoleap-West. *For Chron* 82:159–176.
- 556 Hansen J, Ruedy R, Sato M, Lo K. 2010. Global surface temperature change. *Rev Geophys* 48.
- 557 Harris I, Jones PD, Osborn TJ, Lister DH. 2014. Updated high-resolution grids of monthly climatic  
558 observations --- the CRU TS3.10 dataset. *Int J Clim* 34:623–642.
- 559 Haslinger K, Koffler D, Schöner W, Laaha G. 2014. Exploring the link between meteorological  
560 drought and streamflow: Effects of climate-catchment interaction. *Water Resour Res*  
561 50:2468–2487.
- 562 Huang J-G, Tardif JC, Bergeron Y, Denneler B, Berninger F, Girardin MP. 2010. Radial growth  
563 response of four dominant boreal tree species to climate along a latitudinal gradient in the  
564 eastern Canadian boreal forest. *Global Change Biol* 16:711–731.
- 565 Ibáñez B, Ibáñez I, Gómez-Aparicio L, Ruiz-Benito P, García LV, Marañón T. 2014. Contrasting  
566 effects of climate change along life stages of a dominant tree species: The importance of soil-  
567 climate interactions. *Divers Distrib* 20:872–883.
- 568 IPCC. 2014. Climate Change 2014: Synthesis Report. Contribution of Working Groups I, II and III to  
569 the Fifth Assessment Report of the Intergovernmental Panel on Climate Change [Core Writing  
570 Team, R.K. Pachauri and L.A. Meyer (eds.)]. IPCC, Geneva, Switzerland, 151 pp.

- 571 Ito A, Nishina K, Reyer CPO, François L, Henrot A-J, Guy Munhoven, Jacquemin I, Tian H, Yang J,  
572 Pan S, Morfopoulos C, Betts R, Thomas Hickler, Steinkamp J, Ostberg S, Schaphoff S, Ciais  
573 P, Chang J, Rashid Rafique, Zeng N, Zhao F. 2017. Photosynthetic productivity and its  
574 efficiencies in ISIMIP2a biome models: benchmarking for impact assessment studies. *Environ*  
575 *Res Lett* 12:085001.
- 576 Jacoby GC, D'Arrigo RD. 1995. Tree ring width and density evidence of climatic and potential forest  
577 change in Alaska. *Glob Biogeochem Cycles* 9:227–234.
- 578 Jarvis A, Reuter HI, Nelson A, Guevara E. 2008. Hole-filled SRTM for the globe Version 4, available  
579 from the CGIAR-CSI SRTM 90m Database. <http://srtm.csi.cgiar.org>
- 580 Jaume-Santero F, Pickler C, Beltrami H, Mareschal J-C. 2016. North American regional climate  
581 reconstruction from ground surface temperature histories. *Clim Past* 12:2181–2194.
- 582 Krause C, Luszczynski B, Morin H, Rossi S, Plourde P-Y. 2012. Timing of growth reductions in black  
583 spruce stem and branches during the 1970s spruce budworm outbreak. *Can J For Res*  
584 42:1220–1227.
- 585 Landsberg JJ, Waring RH. 1997. A generalised model of forest productivity using simplified concepts  
586 of radiation-use efficiency, carbon balance and partitioning. *For Ecol Manag* 95:209–228.
- 587 Lapenis AG, Lawrence GB, Heim A, Zheng C, Shortle W. 2013. Climate warming shifts carbon  
588 allocation from stemwood to roots in calcium-depleted spruce forests. *Glob Biogeochem*  
589 *Cycles* 27:101–107.
- 590 Latte N, Lebourgeois F, Claessens H. 2015. Increased tree-growth synchronization of beech (*Fagus*  
591 *sylvatica* L.) in response to climate change in northwestern Europe. *Dendrochronologia*  
592 33:69–77.
- 593 Lavigne MB, Ryan MG. 1997. Growth and maintenance respiration rates of aspen, black spruce and  
594 jack pine stems at northern and southern BOREAS sites. *Tree Physiol* 17:543–551.
- 595 Mann ME, Bradley RS, Hughes MK. 1998. Global-scale temperature patterns and climate forcing over  
596 the past six centuries. *Nature* 392:779–787.
- 597 Ministère des Forêts, de la Faune et des Parcs du Québec (MFFPQ). 2014. Données sur les  
598 perturbations naturelles - Insecte : Tordeuse des bourgeons de l'épinette.

- 599 [https://www.donneesquebec.ca/recherche/fr/dataset/donnees-sur-les-perturbations-naturelles-](https://www.donneesquebec.ca/recherche/fr/dataset/donnees-sur-les-perturbations-naturelles-insecte-tordeuse-des-bourgeons-de-lepinette)  
600 [insecte-tordeuse-des-bourgeons-de-lepinette](https://www.donneesquebec.ca/recherche/fr/dataset/donnees-sur-les-perturbations-naturelles-insecte-tordeuse-des-bourgeons-de-lepinette)
- 601 Misson L. 2004. MAIDEN: A model for analyzing ecosystem processes in dendroecology. *Can J For*  
602 *Res* 34:874–887.
- 603 Natural Resources Canada. 2002. Canada3D, digital elevation model of the Canadian Landmass 30,  
604 [http://geogratis.gc.ca/api/en/nrcan-rncan/ess-sst/aa3dc127-4d10-4c1c-a760-](http://geogratis.gc.ca/api/en/nrcan-rncan/ess-sst/aa3dc127-4d10-4c1c-a760-f19bef14042b.html)  
605 [f19bef14042b.html](http://geogratis.gc.ca/api/en/nrcan-rncan/ess-sst/aa3dc127-4d10-4c1c-a760-f19bef14042b.html). Government of Canada, Natural Resources Canada, Earth Sciences  
606 Sector, Canada Centre for Mapping and Earth Observation, editors.  
607 [http://geogratis.gc.ca/api/en/nrcan-rncan/ess-sst/aa3dc127-4d10-4c1c-a760-](http://geogratis.gc.ca/api/en/nrcan-rncan/ess-sst/aa3dc127-4d10-4c1c-a760-f19bef14042b.html)  
608 [f19bef14042b.html](http://geogratis.gc.ca/api/en/nrcan-rncan/ess-sst/aa3dc127-4d10-4c1c-a760-f19bef14042b.html)
- 609 Navarro-Cerrillo RM, Sánchez-Salguero R, Manzanedo RD, Camarero JJ, Fernández-Cancio Á. 2014.  
610 Site and age condition the growth responses to climate and drought of relict *Pinus nigra*  
611 subsp. *salzmannii* populations in southern Spain. *Tree-Ring Res* 70:145–155.
- 612 Novick KA, Ficklin DL, Stoy PC, Williams CA, Bohrer G, Oishi AC, Papuga SA, Blanken PD,  
613 Noormets A, Sulman BN, Scott RL, Wang L, Phillips RP. 2016. The increasing importance of  
614 atmospheric demand for ecosystem water and carbon fluxes. *Nat Clim Change* 6:1023–1027.
- 615 Ols C, Hofgaard A, Bergeron Y, Drobyshev I. 2016. Previous growing season climate controls the  
616 occurrence of black spruce growth anomalies in boreal forests of Eastern Canada. *Can J For*  
617 *Res* 46:696–705.
- 618 Pan Y, Chen JM, Birdsey R, McCullough K, He L, Deng F. 2011. Age structure and disturbance  
619 legacy of North American forests. *Biogeosciences* 8:715–732.
- 620 Paré D, Bernier P, Lafleur B, Titus BD, Thiffault E, Maynard DG, Guo X. 2013. Estimating stand-  
621 scale biomass, nutrient contents, and associated uncertainties for tree species of Canadian  
622 forests. *Can J For Res* 43:599–608.
- 623 R Core Team. 2015. R: A language and environment for statistical computing. R Foundation for  
624 Statistical Computing, Vienna, Austria. URL <http://www.R-project.org/>
- 625 Raulier F, Bernier PY, Ung C-H. 2000. Modeling the influence of temperature on monthly gross  
626 primary productivity of sugar maple stands. *Tree Physiol* 20:333–345.



- 627 Régnière J, Saint-Amant R, Béchard A. 2014. BioSIM 10 — User’s manual. Natural Resources  
628 Canada, Canadian Forest Service, Laurentian Forestry Centre, Quebec, QC. Inf. Rep. LAU-X-  
629 137E. <ftp://ftp.cfl.scf.mcan.gc.ca/regniere/software/BioSIM/Doc/LAU-X-137E.zip>
- 630 Rennenberg H, Loreto F, Polle A, Brilli F, Fares S, Beniwal RS, Gessler A. 2006. Physiological  
631 responses of forest trees to heat and drought. *Plant Biol* 8:556–571.
- 632 Robitaille A, Saucier J-P. 1998. Paysages régionaux du Québec méridional. [réalisé par la Direction de  
633 la gestion des stocks forestiers et la Direction des relations publiques du Ministère des  
634 ressources naturelles du Québec]. Les Publications du Québec, Sainte-Foy, Québec. 213 pp
- 635 Rossi S, Deslauriers A, Anfodillo T, Carrer M. 2008. Age-dependent xylogenesis in timberline  
636 conifers. *New Phytol* 177:199–208.
- 637 Ryan MG. 1991. Effects of climate change on plant respiration. *Ecol Appl* 1:157–167.
- 638 Schneider U, Becker A, Finger P, Meyer-Christoffer A, Rudolf B, Ziese M. 2015. GPCC Full Data  
639 Reanalysis Version 7.0 at 0.5°: Monthly Land-Surface Precipitation from Rain-Gauges built  
640 on GTS-based and Historic Data.
- 641 Smith NG, Malyshev SL, Shevliakova E, Kattge J, Dukes JS. 2016. Foliar temperature acclimation  
642 reduces simulated carbon sensitivity to climate. *Nat Clim Change* 6:407–411.
- 643 Terrier A, Girardin MP, Périé C, Legendre P, Bergeron Y. 2013. Potential changes in forest  
644 composition could reduce impacts of climate change on boreal wildfires. *Ecol Appl* 23:21–35.
- 645 Trujillo E, Molotch NP, Goulden ML, Kelly AE, Bales RC. 2012. Elevation-dependent influence of  
646 snow accumulation on forest greening. *Nat Geosci* 5:705–709.
- 647 Vaganov EA, Hughes MK, Kirdyanov AV, Schweingruber FH, Silkin PP. 1999. Influence of snowfall  
648 and melt timing on tree growth in subarctic Eurasia. *Nature* 400:149–151.
- 649 Verbyla D. 2015. Remote sensing of interannual boreal forest NDVI in relation to climatic conditions  
650 in interior Alaska. *Environ Res Lett* 10:125016.
- 651 Viereck LA, Johnston WF. 1990. *Picea mariana* (Mill.) B.S.P. Black spruce. In Burns, R. M. and  
652 Honkala, B. H. (technical coordinators), *Silvics of North America, Volume 1. Conifers*.  
653 USDA Forest Service Agriculture Handbook 654, Washington, DC.

- 654 Vlam M, Baker PJ, Bunyavejchewin S, Zuidema PA. 2014. Temperature and rainfall strongly drive  
655 temporal growth variation in Asian tropical forest trees. *Oecologia* 174:1449–1461.
- 656 Wang Y, Hogg EH, Price DT, Edwards J, Williamson T. 2014. Past and projected future changes in  
657 moisture conditions in the Canadian boreal forest. *For Chron* 90:678–691.
- 658 Whitlock MC. 2005. Combining probability from independent tests: the weighted Z-method is  
659 superior to Fisher’s approach. *J Evol Biol* 18:1368–1373.
- 660 Wilson R, D’Arrigo R, Buckley B, Büntgen U, Esper J, Frank D, Luckman B, Payette S, Vose R,  
661 Youngblut D. 2007. A matter of divergence: Tracking recent warming at hemispheric scales  
662 using tree ring data. *J Geophys Res* 112:D17103.
- 663 Wu X, Liu H, Guo D, Anenkhonov OA, Badmaeva NK, Sandanov DV. 2012. Growth decline linked  
664 to warming-induced water limitation in Hemi-Boreal forests. *PLoS ONE* 7(8): e42619. doi:  
665 10.1371/journal.pone.00426
- 666 Wu Z, Ahlström A, Smith B, Ardö J, Eklundh L, Fensholt R, Lehsten V. 2017. Climate data induced  
667 uncertainty in model-based estimations of terrestrial primary productivity. *Environ Res Lett*  
668 12:064013.
- 669 Zang C, Biondi F. 2015. treeclim: an R package for the numerical calibration of proxy-climate  
670 relationships. *Ecography* 38:431–436.
- 671
- 672

Figure legends

**Figure 1.** (a) Location of the black spruce forests under study, eastern Canada. The sampling sites ( $n = 50$ ) are shown accordingly with the positioning of transects along the west to east gradient (*colored symbols*). Slopes of linear trends ( $^{\circ}\text{C}$  per year) in summer (June to August) mean daily maximum temperatures from 1901 to 2013 are shown in background colors. (b) Distribution of sampling sites within gradients of mean annual temperature (MAT,  $^{\circ}\text{C}$ ) and mean annual precipitation total (MAP, mm). The CRU TS 3.22 database (Harris and others, 2014) was used for generating this climate information.

**Figure 2.** Average correlations between monthly climate data and (a) RWI and (b) NPP metrics across all sites over 1908-2013. Analyses were conducted using 21-year-long moving windows incremented in 5-year steps. (c) Comparison of the distributions of correlations obtained in (a) and (b), for each month and period combinations, using a Wilcoxon-Mann-Whitney test. Monthly climate variables included minimum ( $T_{\min}$ ) and maximum ( $T_{\max}$ ) temperatures, and total precipitation (Prec) extracted at site level from the  $0.5^{\circ} \times 0.5^{\circ}$  CRU database (Harris and others 2014). Months spanned from May the year previous to growth to August of the current year. Current year months start with a capital letter. The significance of each averaged correlation across sites was evaluated under two sets of climate-growth hypotheses using one-sided competitive tests (see 2.7 Climate-growth relationships). Open circles and black dots on panels (a) and (b) identify significant ( $P < 0.05$ ) correlations under hypotheses 1-3 and 4-6, respectively. Black dots on panel (c) stand for no significant ( $P > 0.05$ ) differences in the distribution of correlations.

**Figure 3.** (a) Mean of site RWI chronologies above  $51.5^{\circ}\text{N}$ . (b) Mean July-to-September river flow measured at the De Pontois river station ( $53^{\circ}\text{N}$ - $74^{\circ}\text{W}$ , Table S3) over 1960-1993. (c) Biplot of the mean July-to-September De Pontois river flow of the year previous to growth and RWI of the year contemporaneous to growth over 1961-1994. A linear regression with 95 % confidence interval is shown:  $R^2 = 0.24$ . (d) Site-specific correlation between the mean July-to-September De Pontois river

flow and RWI. Blue and red circles represent negative and positive correlations, respectively; the larger the circle, the higher the correlation value. Black contours indicate significant correlations ( $P < 0.05$ ).

**Figure 4.** (a) Average tree-ring width indices (black line) and net primary production (red line) chronologies across all sites ( $n = 50$ ) over 1908-2013. (b) Moving correlations between both metrics were computed using 21-year-long windows incremented in one-year steps. Correlations are plotted on the central year of each interval. Significant correlations ( $P < 0.05$ ) are indicated with black dots.

**Figure 5.** Pearson correlations ( $r$ ) between site-specific RWI and NPP metrics during five different 21-yr periods: (a) 1913-1933, (b) 1933-1953, (c) 1953-1973, (d) 1973-1993, and (e) 1993-2013. Correlations were computed using original (left-hand panels) and first-differenced (right-hand panels) metrics. Blue and red circles represent negative and positive correlations, respectively. The larger the circle, the higher the value of the correlation ( $|r|$ ). Black contours delineating circles indicate significant correlations ( $P < 0.05$ ). Black crosses indicate the position of meteorological stations available for that period.

**Figure 6.** Potential factors involved in the low RWI-NPP correlation from 1953 to 1993. (a) Changes in the median distances of weather stations closest to the sampling site over the years (blue: precipitation; red: temperature), with 95 % confidence intervals computed from exact bootstrap resampling. Lower values denote a densification of the weather station network; higher values denote a scarce weather station network. (b) Vertical bars: percentage of sites located within a defoliated polygon of Quebec's provincial annual surveys covering 1967 to 2006 (source: MFFPQ 2014); the inset map shows the projected defoliated areas from 1974 to 1978 (gray shading) relative to the position of the sampling sites (black dots). Classes denote the percentage of needle loss on the annual shoot: light (1 to 35%), moderate (36 to 70%), and severe (71 to 100%). (c) Site-specific elevation (alt., above sea level) against the standard deviation (SD) of the altitudinal gradients between the four nearest weather stations and each site, as estimated using the software BioSIM over 1953-1993

(Régnière and others 2014). If the four nearest stations did not all present climate records over the entire period, additional stations were added until the full period was covered. Site-specific 1953-1993 RWI-NPP correlations are plotted using transect-specific symbols: circles for West, squares for Central and triangles for East. Blue and red symbols represent negative and positive correlations, respectively; the larger the symbol, the higher the correlation value. Black contours indicate significant correlations ( $P < 0.05$ ). (d) Altitudinal gradient (map) versus the distribution of the 1953-1993 NPP-RWI correlations (Jarvis and others 2008). The larger the circle, the higher the value of the correlation. Note that the altitudinal scale was truncated to 800 m to enhance contrasts between low- and high-altitude sampling sites.

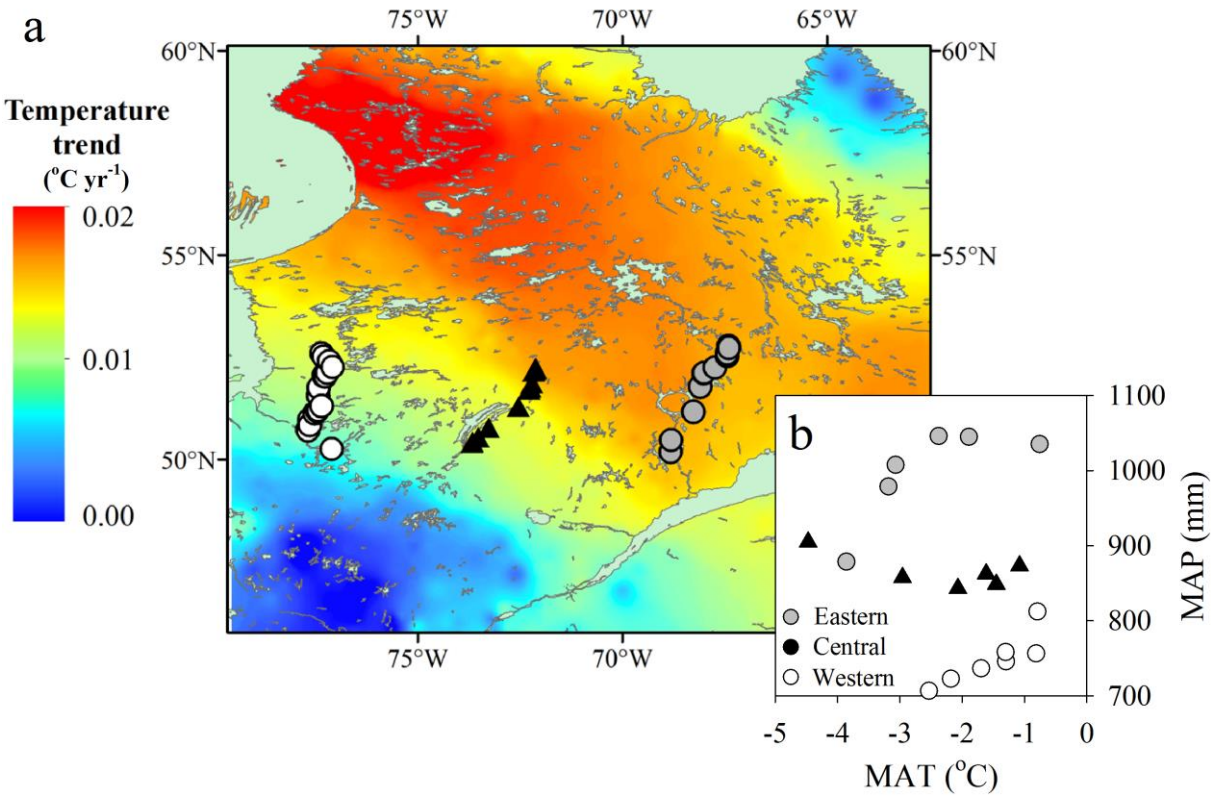


**Figure 1.**

# Shifts in tree growth sensitivity to climate

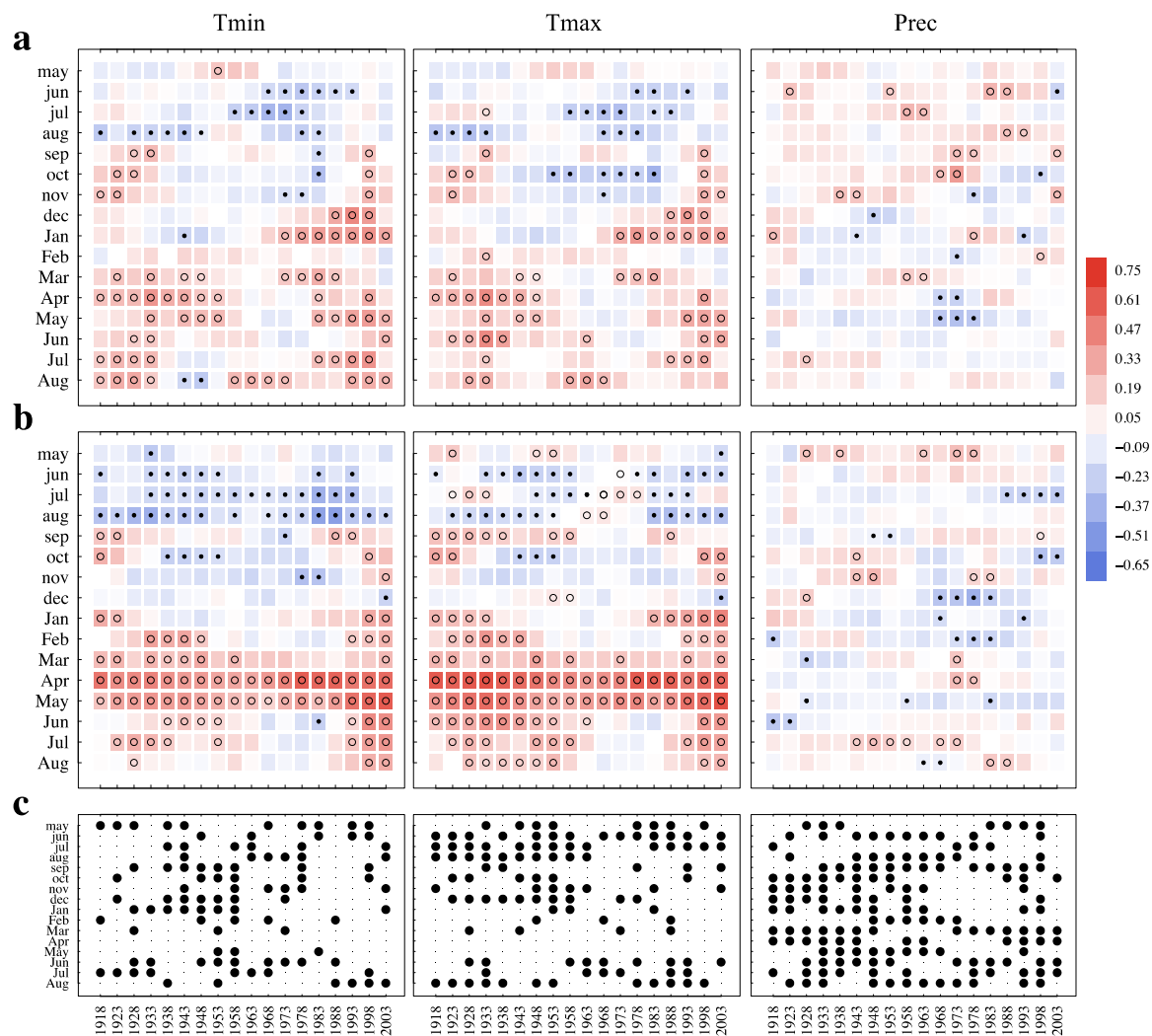


**Figure 2.**

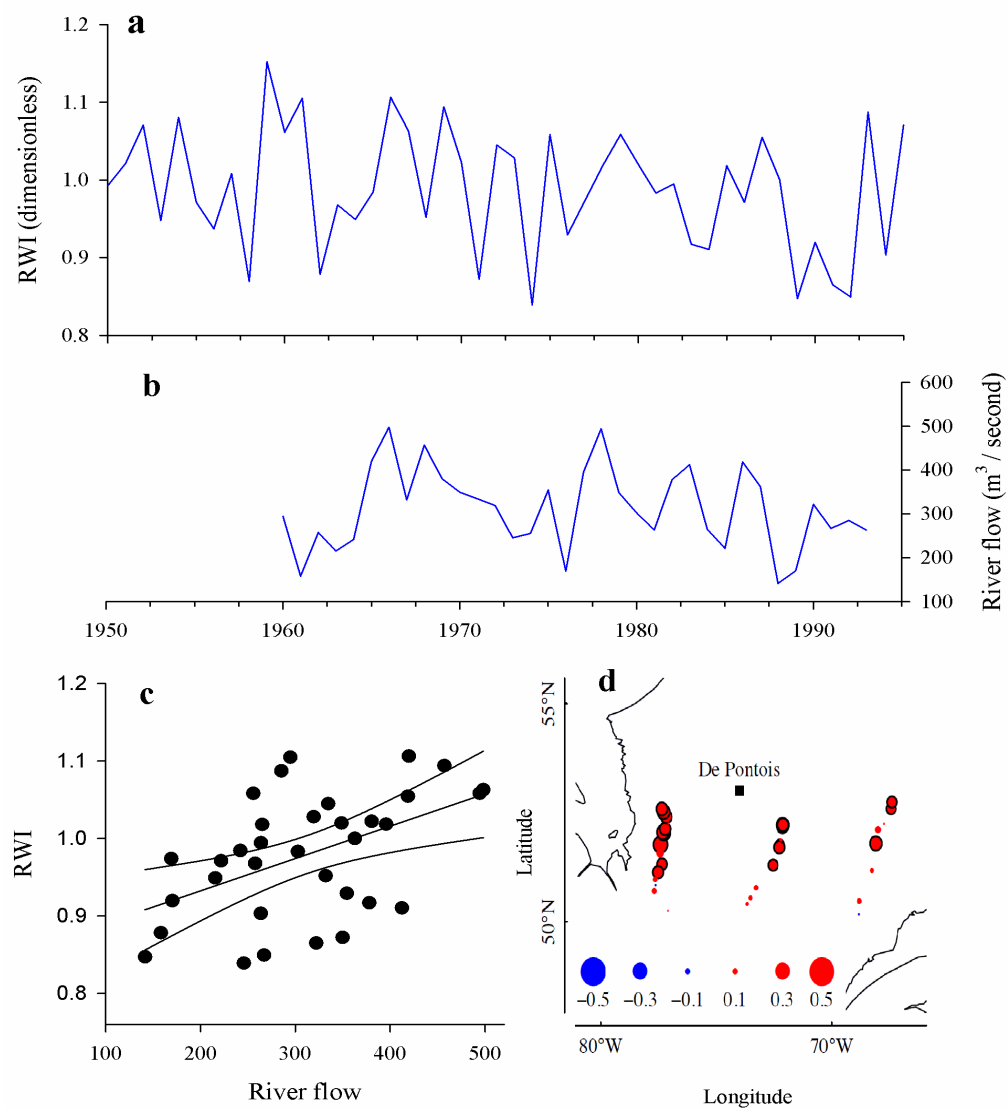


**Figure 3.**



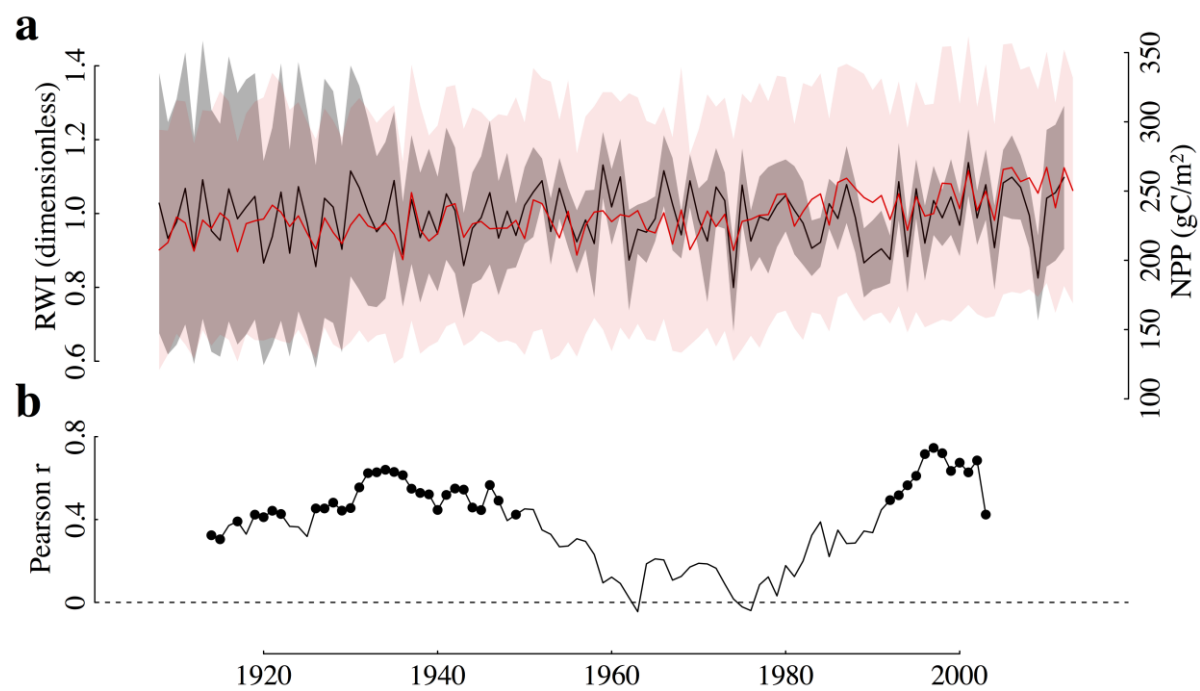


**Figure 4.**

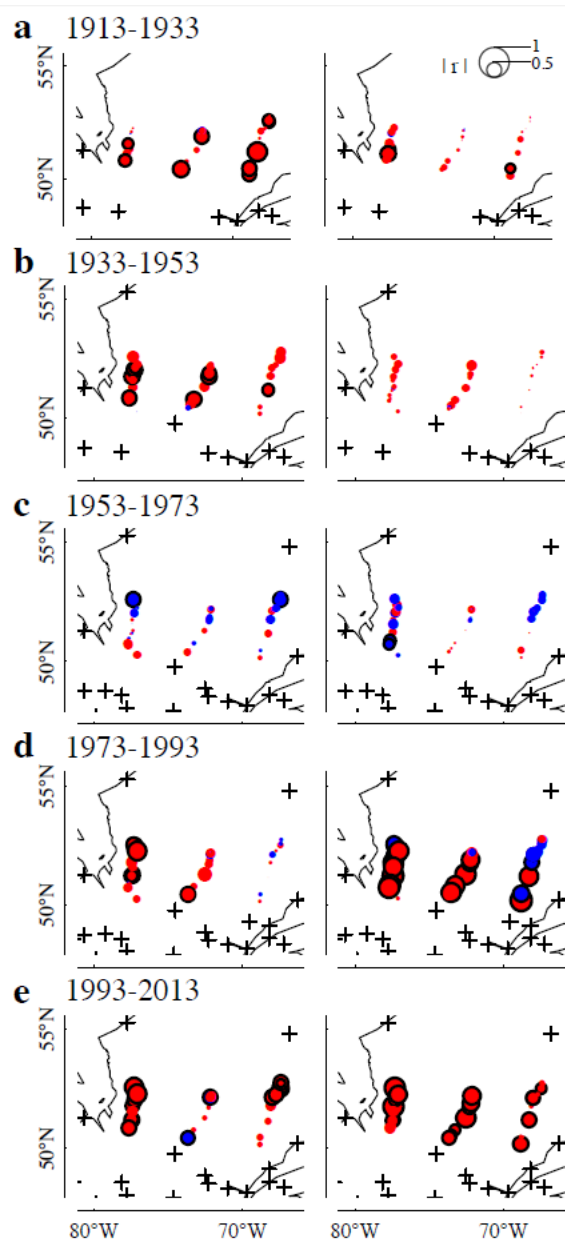


**Figure 5.**

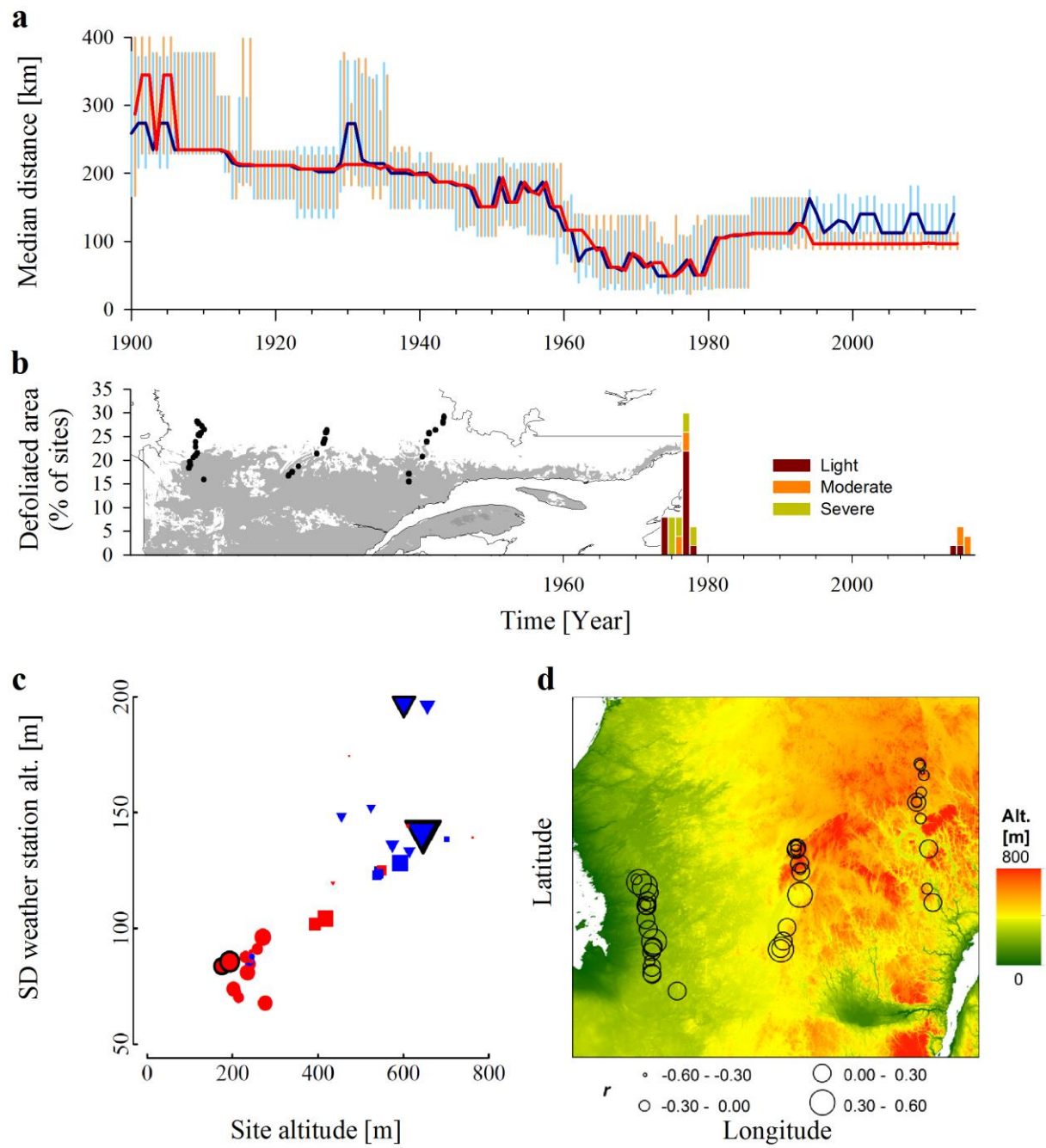


**Figure 6.**